Appl. Phys. B (2013) 112:73–81
DOI 10.1007/s00340-013-5399-0

Applied Physics B
Lasers and Optics

Influence of the retardation of the multiplexing element in a dual channel Q-switched laser

Vid Agrež · Ferdinand Bammer · Boštjan Podobnik · Rok Petkovšek

Received: 21 September 2012 / Accepted: 28 February 2013 / Published online: 31 March 2013

Abstract We present an experimental and numerical analysis, how deviations of the multiplexer-retardation influence the output power of a time-multiplexed dual channel laser. The laser has two different channels, each one with its own gain medium. The channels are time-multiplexed by a single crystal photo-elastic modulator. It enables to double the repetition rate and output power of the laser. However, as multiplexing is based on polarization-switching, the retardation of the modulator should be kept within certain limits. By experimental measurement and theoretical analysis, we determine the operational window within which the retardation should be kept to avoid additional losses into the resonator. The analysis was done for two configurations of the laser setup, namely with and without a quarter-wave plate.

1 Introduction

For many laser micro-processing-based industrial applications the requirements for high processing speeds can be fulfilled by increasing the repetition rate of pulsed lasers. Therefore, for doubling the process speed the repetition rate has to be doubled, too, as well the average power. However, it is also important to keep pulse parameters (pulse duration) constant as one do not want to change the already optimized process but only to speed it up. In general this is complicated, especially in the case of standard solid-state Q-switch lasers. One possible solution represents a dual channel configuration of the laser resonator.

In the past, several dual channel configurations have already been proposed. There were reports on configurations having a single gain medium in the common part of the resonator and two electro-optical or acousto-optical modulators in each channel [1, 2]. For high power applications, the proposed setups were based on two active mediums which can be multiplexed by additional acousto-optical modulators [3]. The purpose of this interesting setup was not power scaling but pulse shaping for laser micro-processing. Furthermore, a configuration for power and repetition rate scaling was also already proposed [4], based on a dual channel resonator and a single electro-optical modulator (EOM). Its task was to switch both channels in turn, therefore to double the frequency and power by summing the laser pulses from each channel. However, despite recent progress in high-voltage high-speed drivers for EOM, this solution seems to be rather cumbersome especially for the high repetition rate (several 100 kHz) typically used in high-speed material processing. The combination of high voltage and high repetition rate requires high power consumption of the driver. As an alternative we have recently demonstrated a new approach based on a single crystal photo-elastic modulator (SCPEM) that can replace the EOM [5]. The main advantage is a relatively simple design that requires almost 1,000 times lower driving voltage and power in comparison to an EOM.

V. Agrež · R. Petkovšek
Faculty of Mechanical Engineering, University of Ljubljana, Aškerčeva 6, 1000 Ljubljana, Slovenia

R. Petkovšek
e-mail: rok.petkovsek@fs.uni-lj.si

F. Bammer (✉)
Institute for Production Engineering and Laser Technology, Vienna University of Technology, Gußhaus-Str. 30, 1040 Vienna, Austria
e-mail: f.bammer@tuwien.ac.at

B. Podobnik
LPKF Laser and Elektronika d.o.o., Polica 33, 4202 Naklo, Slovenia

In our case, the resonator features two channels, each one with a gain medium, combined with a polarizer to a common part of the resonator. The later one includes the out-coupler, a further polarizer, an AOM-Q-switch, and a SCPEM. This is a $LiTaO_3$-crystal, electrically excited on a mechanical resonance, switching the polarization such that both channels are alternately addressed. In most cases, light modulation based on the photo-elastic effect is used for low power applications [6–9]; however, it has been already proven that it can be also used for high power applications, too [10–12].

The proposed dual channel scheme allows to achieve with an existing and well-proved resonator design nearly a doubling of the pulse repetition frequency and of the average power by simply adding an additional resonator channel [5]. This is especially interesting for lasers based on Nd:YVO_4 and Nd:YAG intracavity frequency doubling or tripling [13–17], which are very important for material micro-processing in many areas as for example micro-electronics and photovoltaic industry.

In [5], we introduced the concept and demonstrated a first realization. In this work, we concentrate on the operating window of this channel-switching, which depends on the accuracy of the SCPEM-retardation-amplitude. While this can be set quite precisely in low power applications, significant deviations are to be expected in case of high power operation due to the non-homogenous heating of the crystal, which changes the damping and the optical properties. To prove the robustness of the system, we investigate the influence of the retardation amplitude of the multiplexing element based on a SCPEM on the dual channel laser output. This is important to find out how a potential small deviation from the required retardation amplitude affects the robustness of the concept which is essential for a potential application which requires high stability of laser operation. The work is based on numerical simulation compared with experimental findings and is mainly dedicated to found limits in operation of the laser due to misalignment of polarization controlling components.

2 Theoretical model

The theoretical part of our work introduces a set of laser rate equations with temporal dependency [18–21], including the variations of the inversion population and/or of the photon density along the gain medium [22].

It is important that the model was developed to theoretically investigate an end-pumped solid-state laser, however, it was not supposed to predict the detailed behavior of such kind of laser, which is rather complex. For example, we completely neglected the radial dependence of the beam as well as thermal effects (thermal lensing) that are for example crucial to determine the laser behavior near the threshold, because the laser mirror curvature is optimized for high power operation.

The existing numerical model was rather developed to better understand the effect of an additional optical modulator (SCPEM) inserted inside the laser resonator. Due to deviation from optimum retardation of the modulator the transmission is changed leading to additional losses inside the resonator. The goal of this model is to find out how this affects the laser output.

In our configuration the neodymium, as the active medium, is a four level system. Laser light is emitted between the third and second level with corresponding relaxation time (τ_{32}) around 115 µs. Two other relaxation times are typical for a four level system, namely τ_{43}, τ_{21}, being much smaller, but the corresponding populations cannot be neglected because their values are almost on the same scale as the pulse duration (tens of nanoseconds). The biggest influence, beside relaxation time τ_{32}, on pulse dynamic has the lifetime of lower laser level τ_{21}. For example, if it is increased by factor of two (from 8 to 16 ns) then the laser produces $\sim$10 % shorter pulses, while average power decreases for 2 %. However, τ_{34} has much smaller influence <1 % in pulse width for the same increase.

As a result, the theoretical model consists of five rate equations. Three are describing energy-level occupations and two laser light propagation in positive and negative direction in the crystal. With these we also take into account that Nd:YVO_4 has at given doping (see Table 1) strong absorption and therefore also strong attenuation of the pump light, so we cannot assume uniform gain for laser light through the crystal.

Two more equations for propagation of pumping light could be also added, but this additionally burdens the calculation process. Because we have sufficient ion concentration and the inverse population never exceeds 10 % of its total, we conclude that our approximation is appropriate. The five equations are written as:

$$\frac{\partial N_4}{\partial t} = -\frac{N_4}{\tau_{43}} + \frac{q_4 N_3}{\tau_{43}} + w_p \tag{1}$$

$$\frac{\partial N_3}{\partial t} = -\frac{\sigma_{32} c}{V}(N_3 - N_2)(\phi^+ + \phi^-) - \frac{N_3}{\tau_{32}} - \frac{N_3}{\tau_{31}} - \frac{q_4 N_3}{\tau_{43}} + \frac{N_4}{\tau_{43}} \tag{2}$$

$$\frac{\partial N_2}{\partial t} = +\frac{\sigma_{32} c}{V}(N_3 - N_2)(\phi^+ + \phi^-) - \frac{N_2}{\tau_{21}} + \frac{N_3}{\tau_{32}} \tag{3}$$

$$\pm\frac{\partial \phi^\pm}{\partial z} + \frac{1}{c}\frac{\partial \phi^\pm}{\partial t} = \frac{\sigma_{32}}{V}(N_3 - N_2)(\phi^\pm + S) - \alpha\phi^\pm \tag{4}$$

Equation 4 represents two equations for light propagation in two opposite directions within the active

Table 1 Table of parameters used in the numerical model

Parameter	Value
R_1/R_2	100/80 %
Resonator length L	240 mm
Nd-doping	0.2 %
Gain crystal length	10 mm
Pump power	32 W
Pump beam diameter	1 mm
Laser beam diameter	0.9 mm
Fluorescence lifetime τ_{32}	115 µs
Relaxation time τ_{43}	5 ns
Relaxation time τ_{31}	10 ms
Relaxation time τ_{21}	8 ns
Thermal excitation parameter q_4	1 %
Stimulated emission cross-section σ_{32}	22×10^{-22} m^2 @ 1,064 nm
Averaged absorption coefficient	628 m^{-1} @ 808 nm
Refractive indices of Nd:YVO_4	$n_o = 1.9721$; $n_e = 2.1858$ @ 808 nm
	$n_o = 1.9573$; $n_e = 2.1652$ @ 1064 nm
Peak absorption wavelength	810 nm
Absorption bandwidth (FWHM)	8 nm
Intrinsic losses α	1.8 m^{-1}

medium. Free space propagation is represented by time delay in numerical integration. The ion populations must satisfy $N_t = N_1 + N_2 + N_3 + N_4$, with N_t…total number of active ions. ϕ^+ and ϕ^- represent laser light photons propagating in positive and negative direction, respectively. The parameter q_4 takes thermal excitation from third to fourth level into account.

The emission cross-section is σ_{32}, V represents the volume of the crystal through which laser light is propagating, c is the velocity of light in the medium, and w_p is the pumping rate with a corresponding absorption rate in Table 1, averaged within the FWHM spectrum of the pumping diode (4 nm).

The parameter S is based on semi-classical laser theory and is set to 1. This means that there is one spontaneous photon present in resonator which gets amplified or reabsorbed depending on the sign of gain (i.e., difference of upper and lower laser level populations). This is needed to start laser operation and does then not have any major influence on laser operation.

α represents the intensity loss of laser light in the gain medium.

The reflectivity of the end mirrors and the impact of internal transmission modulation $Q(t)$ due to active optical elements inside the resonators (AOM and SCPEM) are taken into account with the following boundary conditions:

$$\phi^+(z = 0, t) = R_1 \phi^-(z = 0, t) \quad (5)$$

$$\phi^-(z = L, t) = Q(t) R_2 \phi^+(z = L, t), \quad (6)$$

where R_1 and R_2 are left and right mirror reflectivities, respectively. $Q(t)$ is the product of the active elements transmission: Q-switch (based on AOM) and multiplexing modulator (based on SCPEM), respectively:

$$Q(t) = Q_{\mathrm{AOM}}(t) Q_{\mathrm{PEM}}(t) \quad (7)$$

$Q_{\mathrm{AOM}}(t)$ is a trapezoid window with rise/fall times of around 100 ns and transmissions value of 10 and 99 % in closed and open state, respectively. The SCPEM transmission $Q_{\mathrm{PEM}}(t)$ shows two types depending whether an additional quarter-wave plate is used (Eqs. 9, 10). The parameters used in the numerical calculations are listed in Table 1.

Including the longitudinal-dependence of photon- and excitation-densities produce results, which are ~5 % closer to the measurements with respect to the results obtained from the model which consider time dependence only. The radial dependence was neglected, since in our case it does not contribute to any further improvement of the results.

3 Experimental setup

Figure 1a shows the setup of an industrial ns-pulsed laser originally designed for intracavity frequency up conversion. It has a Nd:YVO_4-gain-medium, longitudinally pumped with a diode laser. Q-switching is done with an AOM. Figure 1b shows an expansion of this setup to dual channel operation to increase the average power and repetition rate while maintaining the other pulse parameters (duration and energy) as described in [5]. The laser beams of both channels are combined by a SCPEM-based multiplexing element and a thin film polarizer (POL1). The polarizer transmits the horizontally polarized light of channel 1 and reflects the vertically polarized light of channel 2. In the common laser channel, only horizontal polarization can propagate. The SCPEM in turns rotates the polarization from channel 2 or leaves the polarization of the channel 1 unchanged. This enables light from both channels to propagate in the common resonator channel.

The retardation $\delta(t)$ of the multiplexer consisting of a SCPEM, a polarizer, and an optional λ/4-plate is controlled by an electrically induced mechanical oscillation of the crystal and can be written as:

$$\delta(t) = \delta_0 + \delta_1 \sin(2\pi f_R t) \quad (8)$$

δ_0 corresponds to the static retardation due to wave plate, which is assumed to be zero or equal to π/4 for the configuration with or without the wave plate, respectively.

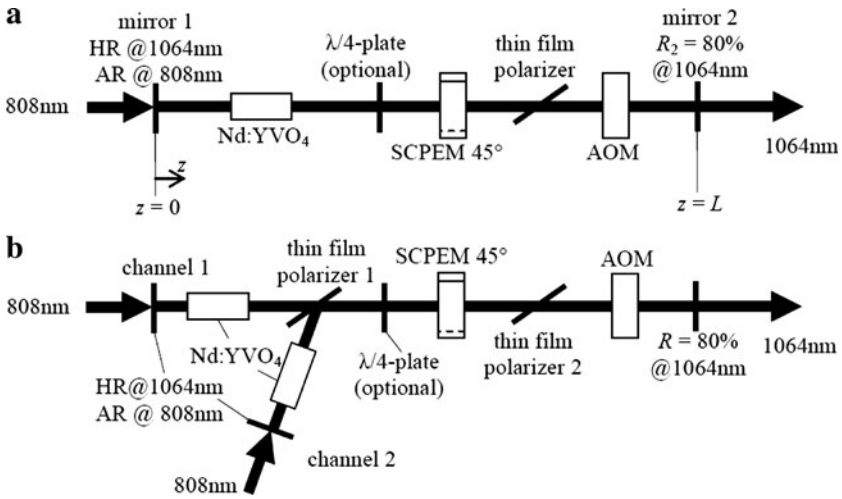

Fig. 1 Basic layout of the laser as modeled by the numerical calculation (**a**). Scheme of the dual channel setup based on a diode-pumped Nd:YVO_4-laser (**b**)

δ_1 is the retardation amplitude of the modulator and f_R is the resonance frequency of the modulator (177.2 kHz in this case). In fact, there is always an additional small offset due to adjustment errors, which is neglected here. The transmission of the SCPEM for channel 1 without a λ/4-plate is:

$$Q_{\mathrm{SCPEM}} = \cos^2\left(\kappa\frac{\pi}{2}\sin(2\pi f_R(t-t_d))\right). \quad (9)$$

With a λ/4-plate we use:

$$Q_{\mathrm{SCPEM}} = \cos^2\left(\frac{\pi}{4}+\kappa\frac{\pi}{4}\sin(2\pi f_R(t-t_d))\right). \quad (10)$$

The retardation amplitudes $\delta_1 = \kappa\pi$ and $\delta_1 = \kappa\pi/2$ are used in Eqs. 9 and 10, respectively. The time t_d is the delay time between the center of the Q-switch window and the center of the SCPEM window. κ represents the relative retardation amplitude in relation to the optimal retardation amplitude. It can vary during laser operation up to ±10 %; however, it can be stabilized by a feedback loop within ±0.5 %. Relative retardation amplitude $\kappa = 1$ means that the retardation amplitude δ_1 for the case without λ/4-plate and case with λ/4-plate is exactly π and π/2, respectively. A similar set of equations can be obtained for the transmission of channel 2 which corresponds to transmission between perpendicular polarizers and therefore the polarization has to be rotated for 90° to have maximum transmission.

Figure 2 shows the transmission curves of the SCPEM for the four cases: without or with λ/4-plate, both for channel 1 or channel 2 (i.e., transmission and reflective mode). Figure 2a and b corresponds to the example without λ/4-plate and show the transmission for channel 1 and channel 2, respectively. They show a highly asymmetric response for the two channels. Channel 2 has a significantly broader transmission window in comparison to channel 1. The high sensitivity to a potential deviation from the optimal retardation amplitude of (i.e., $\kappa = 0.7$ and 1.3) that leads to a relative high deviation of the transmission is further significant. The transmission at the centre of the transmission window of channel 2 drops by 21 %. However, there is only a small effect on the transmission window of channel 1: the width of the window slightly changes. It turns out that this effect has no measurable influence on the laser behavior.

Figure 2c and d shows the situation with a λ/4-plate and represents the transmission of channel 1 (c) and channel 2 (d) showing completely symmetric response. Further the same relative deviation from the retardation amplitude as mentioned above (i.e., $\kappa = 0.7$ and 1.3) has much smaller effect on transmission (drop of 5.5 %) and the effect is the same for both channels. Furthermore, the switching frequency is by a factor 2 smaller than in the case without retarder.

The overall transmission of one single channel depends on the SCPEM and on the AOM. They must be precisely synchronized to Q-switch each laser channel. The principle of operation can be explained as follows. As previously mentioned, the SCPEM alternately selects channel 1 and 2, however, only when the AOM is simultaneously open the selected channel is in a transmission state and emits a laser pulse. The repetition rate is therefore still controlled by the AOM as in the original single channel version. However, due to the fixed frequency of the SCPEM, only discrete values of the output repetition rate are possible. The available repetition rates are $f = 4f_R/(2n-1)$ without λ/4 plate and half of that $f = 2f_R/(2n-1)$ with the plate, where n is a positive integer. With $f_R = 177.2$ kHz these useful repetition rates for micro-processing (approx. range 50–250 kHz) are: 236, 142, 101, 79, 64, 55, and 118, 71, 51 kHz for the setup without or with retarder, respectively.

Figure 3 shows the resulting overall transmission for channel 1 for three different retardation amplitudes. It is

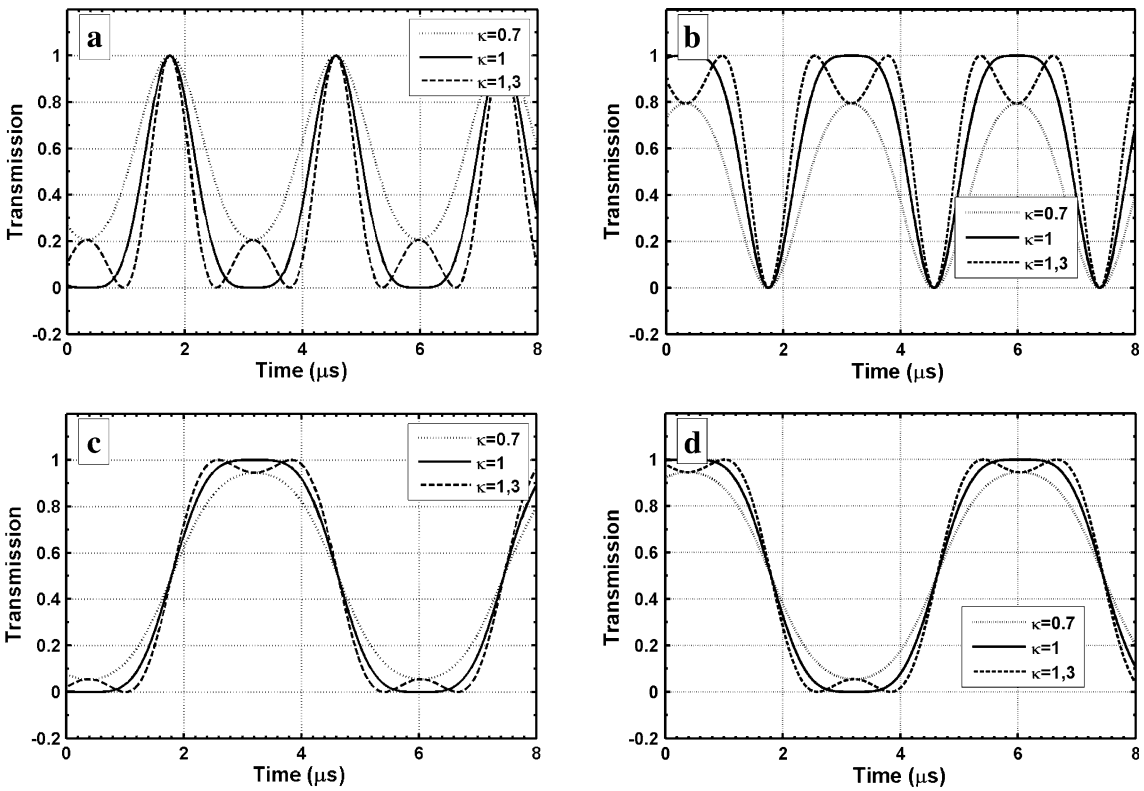

Fig. 2 The SCPEM can operate without (graph **a** and **b**) or with (graph **c** and **d**) the λ/4-plate. The graphs on the *left* (**a** and **c**) and on the *right* (**b** and **d**) show the transmission curve for channel 1 and channel 2, respectively. The *solid line* represents transmission in the case of the ideal retardation amplitude ($\kappa = 1$). The *dotted* and *dashed line* corresponds to a deviation of -30 and $+30$ % (i.e., $\kappa = 0.7$ or $\kappa = 1.3$) from the ideal retardation amplitude, respectively

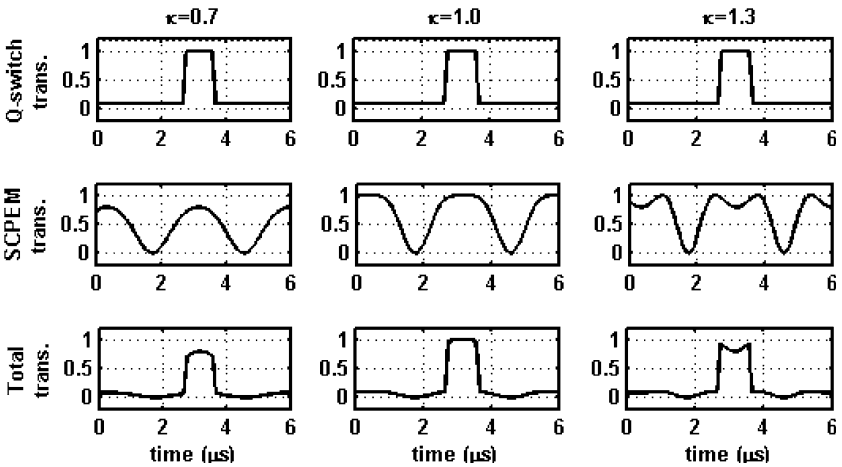

Fig. 3 Transmission of the combination of AOM-Q-switch and SCPEM for the case without λ/4 wave plate ($\delta_0 = 0$). The *upper graphs* represent the AOM-transmission. The *middle row* shows the SCPEM transmission for channel 1 for three different retardation amplitudes: $\delta_1 = 0.7\pi$, π, and 1.3π. The *lower row* of graphs represents the resulting transmission of both

clear that a deviation from ideal retardation ($\kappa = 1$) of the SCPEM modulator leads to a lower total transmission. Consequently, the resonator exhibits higher loss and the output power is decreased. However, in case of higher retardation amplitude ($\kappa > 1$) the effect can be compensated by changing the delay between the SCPEM and the AOM Q-switch.

4 Results and discussion

In order to adapt the theoretical model to the measurements we used two parameters: the overlap of the pumping beam with the signal beam and the losses inside the resonator (mainly due to the insertion of additional optical elements needed for channel switching). With the values given

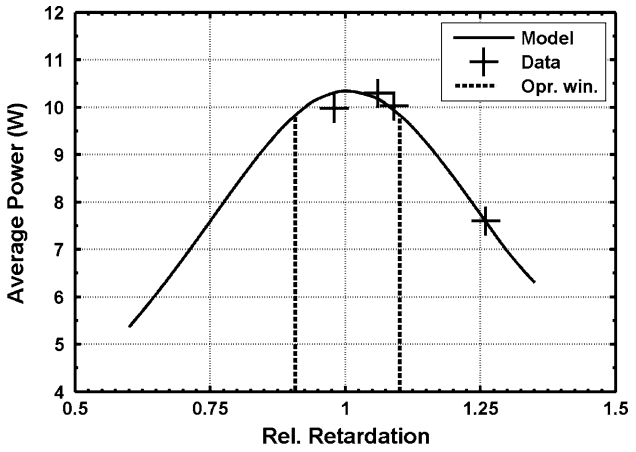

Fig. 4 Dependence of average power on relative retardation amplitude and operating window for the setup without λ/4-plate for channel 2. There is no dependence on retardation amplitude for the channel 1 (*see text*). We estimate the error of the measurement to 4–5 %

below a reasonable agreement regarding average output power was observed.

- From fitting in our theoretical model we get 78 % overlap between pumping light and laser light, which fit well to the geometrical estimation (∼80 %).
- Losses in the resonator (channel 2):

  a. 5.0 % for all losses + SCPEM without $\lambda/4$ retarder,
  b. 6.5 % for all losses + SCPEM with $\lambda/4$ retarder.

The losses for channel 1 are approximately 2 % higher, mainly due to higher losses on the thin film polarizer 1 which for this channel operates in transmission mode in comparison with channel 2 operating in reflective mode.

The dependence of the average power on relative retardation obtained from the measurement and from the theoretical model is presented in Fig. 4 (no λ/4-plate) and Fig. 5 (with λ/4-plate). For the case without λ/4-plate only data for channel 2 are shown because we did not observe any measurable dependence on retardation amplitude for channel 1. It can be explained by the fact that the SCPEM transmission window for this channel shows almost no dependence on retardation amplitude as it is clear from Fig. 2a. However, the output power of channel 1 is approximately 0.5 W lower in comparison with channel 2 due to higher loss. From the theoretical curve one can estimate the operating window, within which the output power does not decrease more than 5 %, that roughly corresponds to the relative change of the retardation amplitude of ±10 %. These numbers do not represent limits for short-term stability, but should be considered as an effect due to aging or for example batch to batch difference during potential production.

Results for the setup with λ/4-plate are shown in Fig. 5. In this case, due to symmetric transmission curves of the modulator (Fig. 2c, d) also the curves for average output power for channel 1 and 2 are similar. However, the average power of channel 1 is slightly lower in comparison to channel 2 due to higher losses. The operating window is in this case much broader and corresponds to a relative change of the retardation amplitude of approximately ±20 %. This is expected as in this case half of retardation amplitude necessary for polarization rotation comes from the $\lambda/4$-retarder and only half came from the modulator. Consequently, this configuration is less sensitive to a relative change of modulator retardation.

In general, one can conclude that in both cases the setup is relatively robust allowing a relatively broad operating

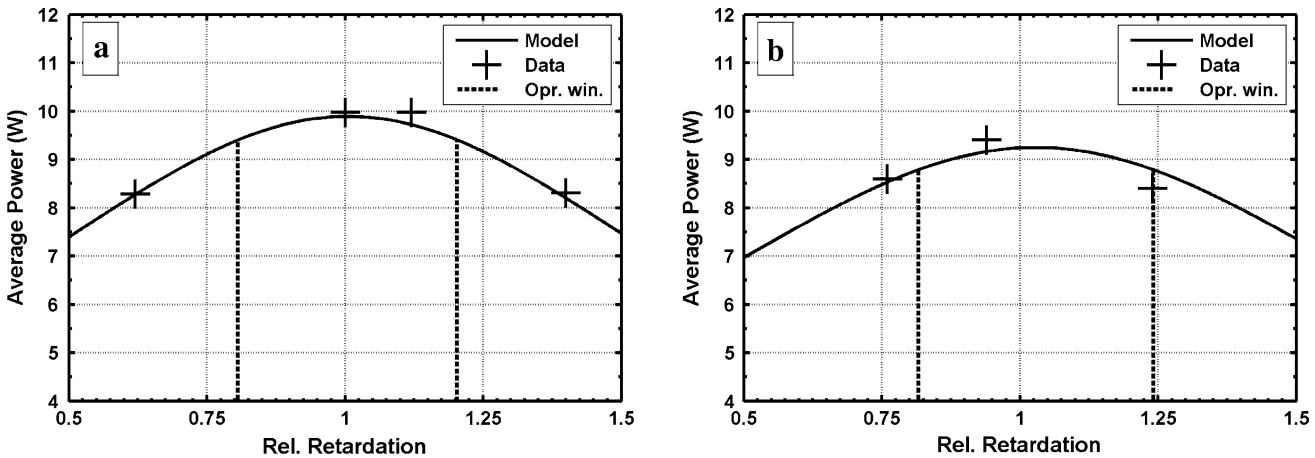

Fig. 5 Dependence of average power on relative retardation amplitude and operating window for the setup with λ/4-plate. The average power of channel 2 (**a**) is slightly higher in comparison to channel 1 (**b**) due to lower losses

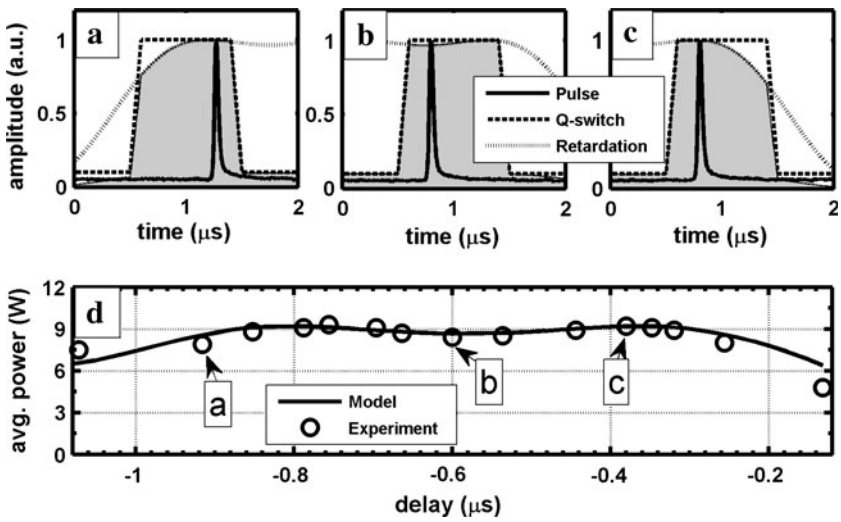

Fig. 6 Dependence of average power on the delay of Q-switch for relative retardation $\kappa = 1.24$ (graph **d**). The *upper* three graphs **a**, **b** and **c** represent three typical points from the main graph (**d**) (*see text*). The *upper* three graphs are numerical simulations

Table 2 Output power for $t_d = 0$ and maximum output power for few selected relative retardation amplitudes κ for the setup without λ/4-plate for reflection mode (channel 2)

	K	Model			Measurement		
		$P_{avg}(t_d = 0)$ (W)	$P_{avg}(t_d)$ (W)	t_d (μs)	$P_{avg}(t_d = 0)$ (W)	$P_{avg}(t_d)$ (W)	t_d (μs)
No λ/4 plate—reflection mode	0.98	10.32	10.32	0.0	9.97	9.97	0.0
	1.06	10.18	10.29	0.29	10.3	10.3	0.0
	1.09	9.95	10.25	0.29	10.0	10.3	0.34
	1.26	7.61	10.02	0.58	7.6	10.2	0.54

The time delay required to obtain maximum power is also indicated

window. The setup with λ/4-plate seems to be more robust not only due to the wider operating window, but also due to lower retardation amplitude required for operation (lower driving voltage!). On the other hand, it needs an additional optical element and consequently exhibits higher losses that lead to slightly lower output power (4 %).

The operating window and therefore the robustness of the system can be further increased by a precise temporal synchronization of the Q-switch pulse and modulator driving signal. In the case when the retardation amplitude is too low or too high the total transmission determined by modulator and Q-switch is decreased (see Fig. 3). As already shown it results in decreased output power. However, if the retardation is too high it is still possible to regain the power by delaying the Q-switch pulse in respect to modulator waveform. The effect of the Q-switch pulse delay on laser pulse build up and output power is presented in Fig. 6 for the case with λ/4-plate and the relative retardation amplitude $\kappa = 1.24$. The lower graph shows the relation between output power and time delay. A delay $t_d = 0$ corresponds to the reference point for ideal retardation amplitude ($\kappa = 1.0$ and consequently $\delta(t) = \pi$) and perfect synchronizations of the electrical control signals of SCPEM and AOM.

Figure 6a, b and c represents the pulse built up for three typical delays from Fig. 6d for a relative retardation amplitude $\kappa = 1.24$ and for the case with λ/4-plate. Figure 6a shows the case when the Q-switch pulse appears too early (delay of −0.80 μs) with respect to the modulator waveform, hence before the modulator reaches its maximum transmission. Due to higher losses at the beginning of the Q-switch the laser pulse appears at the end of the Q-switch window (or pulse) and the output power is decreased. Figure 6b shows the position of a pulse when it is aligned with the retardation dip (delay 0 μs). Due to decreased transmission at the center of the modulator pulse the output power is decreased, too. Finally, Fig. 6c shows an example where the Q-switch pulse is aligned with one modulator transmission maximum (delay of +0.53 μs). In this case, the output power is maximum for the given relative retardation and is almost equal to the value of the optimal condition ($\kappa = 1$, $t_d = 0$). Of course the output power can be regained only in the case when relative retardation is $\kappa > 1$. An overview of the maximum output power for few selected relative retardation amplitudes is given in Tables 2 and 3 for the setup without and with λ/4-plate,

Table 3 Output power for $t_d = 0$ and maximum output power for few selected relative retardation amplitudes κ for the setup with λ/4-plate in reflection and transmission mode

	K	Model			Measurement		
		$P_{avg}(t_d = 0)$ (W)	$P_{avg}(t_d)$ (W)	t_d (μs)	$P_{avg}(t_d = 0)$ (W)	$P_{avg}(t_d)$ (W)	t_d (μs)
λ/4-plate—transmission mode	0.76	8.62	8.62	0.0	8.6	8.6	0.0
	0.94	9.20	9.20	0.0	9.4	9.4	0.0
	1.24	8.67	9.19	0.55	8.4	9.2	0.53
λ/4-plate—reflection mode	0.62	8.22	8.22	0.0	8.28	8.28	0.0
	1.00	9.89	9.89	0.0	9.97	9.97	0.0
	1.12	9.72	9.86	0.42	9.97	10.2	0.33
	1.40	8.28	9.78	0.69	8.31	10.1	0.61

The time delay required to obtain maximum power is also indicated

respectively, for the repetition rate of 118 kHz. The time delay required to obtain maximum power is also indicated.

However, it should be mentioned that for the setup without λ/4-plate due to asymmetry of the channels only pulses from one channel have to be delayed. It results in a non-uniform pulse distribution in time domain what could be an obstacle for some specific applications (e.g., thin film processing). On the other hand, for the setup with λ/4-plate due to channel symmetry the pulses still remain uniformly distributed. There is also no significant difference in pulse widths for all cases presented in the Tables 2 and 3. However, our model predicts slightly shorter widths (39–41 ns) in comparison to ones obtained from the measurement (43 ± 2 ns).

5 Conclusion

We have demonstrated a numerical simulation and experimental study of a dual channel laser. The study focused on the potentially unwanted effects of the retardation error of the multiplexing element and its potential influence on the output power of the laser. The possible configurations are presented with and without an additional λ/4-plate. We have shown that with a λ/4-plate the system is less sensitive to the relative change of the modulator retardation; however, the additional element in the resonator makes it more complex and increases losses. Therefore, the operational window is larger but in general the output power is slightly lower. We have also shown that the operational window can be further increased by changing the delay time between the AOM-Q-switch and the SCPEM-time-multiplexer driving signal.

Acknowledgments Parts of this work were supported by the EU-funded FP7 ALPINE Project, n. 229231 and by the Slovenian Research Agency (projects L2-2323 and L2-4174).

References

1. B.C. Johnson, R. Herbst, Laser resonator with laser medium exhibiting thermally induced birefringence. Patent, A2 0 370 620 (1990)
2. C. Naiman, S. Pompian, Multi-color, multi-pulse laser. Patent, US 6.199.794 (2001)
3. L. Sun, Y. Sun, Methods and systems for synchronized pulse shape tailoring. Patent, WO 2006/062744 A2 (2006)
4. B. Kmetec, B. Podobnik, G. Kusnezow, Mehrkanaliger laser. Patent, DE 10 2007 002 472 A1 (2008)
5. R. Petkovšek, V. Novak, F. Bammer, J. Možina, B. Podobnik, Power scaling of AOM-switched lasers with SCPEM-based time-multiplexing. Opt. Express **19**(21), 19855–19860 (2011)
6. A. Zeng, F. Li, L. Zhu, H. Huang, Simultaneous measurement of retardance and fast axis angle of a quarter-wave plate using one photoelastic modulator. App. Opt. **50**(22), 4347–4352 (2011)
7. D.J. Diner, A. Davis, B. Hancock, S. Geier, B. Rheingans, V. Jovanovic, M. Bull, D.M. Rider, R.A. Chipman, A.-B. Mahler, S.C. McClain, First results from a dual photoelastic-modulator-based polarimetric camera. App. Opt. **49**(15), 2929–2946 (2010)
8. H.-M. Tsai, C.-W. Chen, T.-H. Tsai, Y.-F. Chao, Deassociate the initial temporal phase deviation provided by photoelastic modulator for stroboscopic illumination polarization modulated ellipsometry. Rev. Sci. Instr. **82**(3), 35117 (2011)
9. R. Petkovšek, J. Petelin, J. Možina, F. Bammer, Fast ellipsometric measurements based on a single crystal photo-elastic modulator. Opt. Express **18**(20), 21410–21418 (2010)
10. F. Bammer, R. Petkovsek, Q-switching of a fiber laser with a single crystal photo-elastic modulator. Opt. Express **15**(10), 6177–6182 (2007)
11. F. Bammer, R. Petkovsek, M. Frede, B. Schulz, Q-switching with a dual mode single crystal photo-elastic modulator. SPIE Proc. **7131**, H1–H4 (2008)
12. R. Petkovšek, J. Saby, F. Salin, T. Schumi, F. Bammer, SCPEM-Q-switching of a fiber-rod-laser. Opt. Express **20**(7), 7415–7421 (2012)
13. H. Zhang, P. Shi, D. Li, K. Du, Diode-end-pumped, electro-optically Q-switched Nd:YVO4 slab laser and its second-harmonic generation. App. Opt. **42**(9), 1681–1684 (2003)
14. S. Zhang, L. Guo, B. Xiong, Y. Liu, W. Hou, X. Lin, J. Li, High electro-to-optical efficiency 180 W Q-switched 532 nm laser with a pulsewidth of 70 ns. Appl. Phys. B—Lasers Optics **104**(4), 861–866 (2011)
15. S. Ding, P. Wang, X. Qing, J. Zhang, S. Wang, X. Zhang, Analysis of actively Q-switched intracavity frequency-doubled

solid-state yellow Raman lasers. Appl. Phys. B—Lasers Optics **104**(4), 819–827 (2011)
16. J. Yi, H.J. Moon, J. Lee, Diode-pumped 100-W green Nd-YAG rod laser. App. Opt. **43**(18), 3732–3737 (2004)
17. C. Stolzenburg, A. Giesen, F. Butze, P. Heist, G. Hollemann, Cavity-dumped intracavity-frequency-doubled Yb-YAG thin disk laser with 100 W average power. Opt. Lett. **32**(9), 1123–1125 (2007)
18. J.H. Garcıa-López, V. Aboites, A.V. Kir'yanov, M.J. Damzen, A. Minassian, High repetition rate Q-switching of high power Nd:YVO4 slab laser. Optics Commun **218**(1–3), 155–160 (2003)
19. J.H. Liu, C.Q. Wang, C.L. Du, L. Zhu, H.J. Zhang, X.L. Meng, J.Y. Wang, Z.S. Shao, M.H. Jiang, High-power actively Q-switched Nd:GdVO4 laser end-pumped by a fiber-coupled diode-laser array. Optics Commun. **188**(1–4), 155–162 (2001)
20. K.J. Yang, S.Z. Zhao, G.Q. Li, H.M. Zhao, Theoretical and experimental study of a laser-diode-pumped actively Q-switched Nd:YVO4 laser with acoustic-optic modulator. Optics Laser Technol. **37**(5), 381–386 (2005)
21. X.Y. Zhang, S.Z. Zhao, Q.P. Wang, B. Ozygus, H. Weber, Modeling of diode-pumped actively Q-switched lasers. IEEE J. Quantum Electron. **35**(12), 1912–1918 (1999)
22. Y.F. Chen, Y.P. Lan, S.C. Wang, Modeling of diode-end-pumped Q-switched solid-state lasers: influence of energy-transfer up conversion. J. Opt. Soc. Am. B—Opt. Phys. **19**(7), 1558–1563 (2002)